Journal of Nuclear Materials 386–388 (2009) 26–29

Contents lists available at ScienceDirect

Journal of Nuclear Materials

journal homepage: www.elsevier.com/locate/jnucmat

Atomistic simulation of single kinks of screw dislocations in α-Fe

Lisa Ventelon *, F. Willaime, P. Leyronnas

Service de Recherches de Métallurgie Physique, CEA/Saclay, 91191 Gif-sur-Yvette, France

A B S T R A C T

We have studied the structure and the formation and migration energies of single kinks in ½⟨1 1 1⟩ screw dislocations in body-centered cubic iron, by performing static calculations using the Ackland–Mendelev empirical potential, which correctly accounts for the non-degenerate core structure. The methodology for constructing simulation cells with fully periodic boundary conditions based on the quadrupolar arrangement of dislocation dipoles, with a single kink on each dislocation line is presented. The two types of kinks – left and right – are found to have similar widths, namely ~20 Burgers vectors. The convergences of the formation energies with cell-size along the dislocation line, as well as with the distance between the two dislocations are investigated. A dependence proportional to the inverse of the distance between kinks along the dislocation line is found when kinks overlap. The formation energies of the left and right kinks are significantly different: 0.57 and 0.08 eV, respectively. The Peierls potentials of the second kind are evaluated with the drag method: the energy barriers are found to be lower than 0.1 meV for both kinks.

1. Introduction

Screw dislocation glide is obtained by two processes at finite temperature: the nucleation of kink-pairs within a straight dislocation lying in a single Peierls valley, and the propagation of the kinks along the dislocation line. These phenomena have been recently investigated using atomistic dynamic simulations in body-centered cubic (bcc) iron [1,2]. In the present paper, empirical potential calculations are performed to characterize the static properties of the kinked ⟨1 1 1⟩ screw dislocations. This study is based on the Ackland–Mendelev empirical potential [3], which was shown to correctly reproduce the non-degenerate core structure predicted by density functional theory (DFT) calculations in iron, among the two possible core structures [2,4–6]. This paper focuses on the methodology for setting up fully periodic simulation cells to perform accurate energy calculations on single kinks.

2. Methodology

For this study, we have chosen to consider a dislocation dipole in a periodic supercell [7]. The cartesian axes, x, y and z, are taken, respectively, along the $[\bar{1}\,2\,\bar{1}]$, $[\bar{1}\,0\,1]$ and $[1\,1\,1]$ directions. The Burgers vectors are $\pm\frac{1}{2}[1\,1\,1]$. The first two cell vectors, C_1 and C_2, are chosen to generate a square-like periodic array of dislocation quadrupoles in the (x,y) plane [8]. Following Ref. [7], pre-tilt components in the z direction are added to C_1 and C_2 to accommodate for the plastic strain generated by the straight dislocation dipole. For a straight dislocation the third cell vector, C_3, is taken along z.

Let us now consider how to deal with single kinks. There are two families of kinks for a ⟨1 1 1⟩ screw dislocation in a bcc lattice, referred to as left and right kinks [9]. They can be distinguished by looking at their effect on the [1 1 1] row of atoms which is next to both dislocation positions, as illustrated in Fig. 1(a) and (b). The two parts of the atomic rows get either closer to each other by $b/3$, or separated by the same amount; for this reason the two types of kinks are also called interstitial and vacancy type [1]. It is straightforward to set up a simulation cell containing either a kink-pair, i.e. two segments of opposite-sign edge dislocations, or three kinks of the same sign [10]: the double-kink satisfies the periodicity along the [1 1 1] direction while, in the three kink configuration, a $\pm[\bar{1}\,2\,\bar{1}]$ component, corresponding to the sum of the three kink vectors is added to C_3. The difficulty for adding a single kink per dislocation line arises from the fact that the kink vector $\pm 1/3[\bar{1}\,2\,\bar{1}]$ is not a periodic vector of the perfect crystal. Noticing that $\pm 1/3[\bar{1}\,2\,\bar{1}] \mp 1/6[1\,1\,1]$ is a periodicity vector, the solution for overcoming this difficulty is to essentially remove or add one (1 1 1) layer of atoms (or more generally the atoms contained within the sub-cell formed by C_1, C_2 and $1/6[1\,1\,1]$). The component $\pm 1/3[\bar{1}\,2\,\bar{1}] \mp 1/6[1\,1\,1]$ is then simply added to C_3, as illustrated in Fig. 2. The tilt components have been deduced in previous studies from elasticity calculations for the perfect dislocation within the quadrupolar arrangement [5,8] and are summarized in Table 1, along with the components that are deduced from the bcc geometry and necessary to apply periodic boundary conditions to the cell with a single kink on each dislocation. A perfect agreement is obtained between the formation energies computed from either

* Corresponding author.
E-mail address: lisa.ventelon@cea.fr (L. Ventelon).

0022-3115/$ - see front matter © 2009 Elsevier B.V. All rights reserved.
doi:10.1016/j.jnucmat.2008.12.053

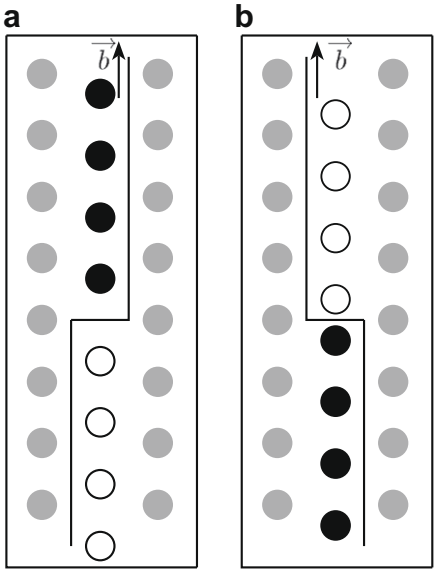

Fig. 1. Schematic representation of the right (or vacancy) kink (a) and the left (or interstitial) kink (b) in a ⟨1 1 1⟩ screw dislocation in the bcc lattice before relaxation; their respective effects are shown on the most affected [1 1 1] row of atoms, represented by black and white spheres. The distance between the upper and lower parts of the row is either increased or decreased by $b/3$. The atoms of the two neighbouring [1 1 1] rows in the same $(\bar{1}01)$ plane (in grey) are represented at their positions for a straight dislocation at the halfway position.

the single-kink simulation cells or the cells with three single-kicks or a kick-pair on each dislocation. The present construction is therefore validated. It has the major advantage of reducing the number of atoms necessary for the computation of single-kink properties by a factor of three. The two dislocations have opposite Burgers vectors, and it can be shown that adding the same kink vector to both dislocation lines yields the same type of kink (either left or right) for both dislocations. The properties of a given type of kink can therefore be deduced separately. The formation energy of a single kink is calculated as the difference between the energy of a kinked screw-dislocation and the energy normalized to the same number of atoms of a straight dislocation lying in a single Peierls valley.

Table 1
Components of the cell vectors, C_1^x, C_1^z, C_2^z, C_3^x and C_3^z, for the different types of cells used for the bulk configuration, and for both perfect dislocation and kinked dislocation. The x and z components are respectively in units of $\sqrt{6}/3a$ and $b=\sqrt{3}/2a$, where a is the cubic lattice parameter. $C_1^y=0$; $|C_2^y|\approx|C_2^x|=|C_1^x|/2\sqrt{a^2+b^2}$; n is an integer chosen such that $C_1^x/(\sqrt{6}a/3)$ is an odd integer; x is along the $[\bar{1}2\bar{1}]$ direction and z is along the [1 1 1] direction.

C_1^x	C_1^z	C_2^z	C_3^x	C_3^z
Bulk				
$3n-1$	+1/3	−1/3	0	0
$3n$	0	0	0	0
$3n+1$	−1/3	+1/3	0	0
Dislocation				
$3n-1$	+1/3	+1/6	0	0
$3n$	0	+1/2	0	0
$3n+1$	−1/3	−1/6	0	0
Right kink				
$3n-1$	+1/3	+1/6	+1	−1/3
$3n$	0	+1/2	+1	−1/3
$3n+1$	−1/3	−1/6	+1	−1/3
Left kink				
$3n-1$	+1/3	+1/6	−1	−2/3
$3n$	0	+1/2	−1	−2/3
$3n+1$	−1/3	−1/6	−1	−2/3

Note that since the dislocation core is non-degenerate with Ackland–Mendelev potential – in agreement with DFT calculations – each type of kink (right or left) has only one possible geometry. This contrasts with previous atomistic studies on kinks in bcc metals, which were based on empirical potentials yielding degenerate cores. In the latter case there are six non equivalent kinks and two so-called flip defects [11–16]. From this point of view, the present results are expected to be much more realistic. However some limitations of the Ackland–Mendelev potential must be kept in mind: compared to DFT calculations, it underestimates the Peierls energy by at least a factor of two, and it yields a double-hump Peierls potential instead of a single hump one [5]. The present results can therefore not be considered as quantitative predictions, and in particular the kink width is likely to be largely overestimated. A more

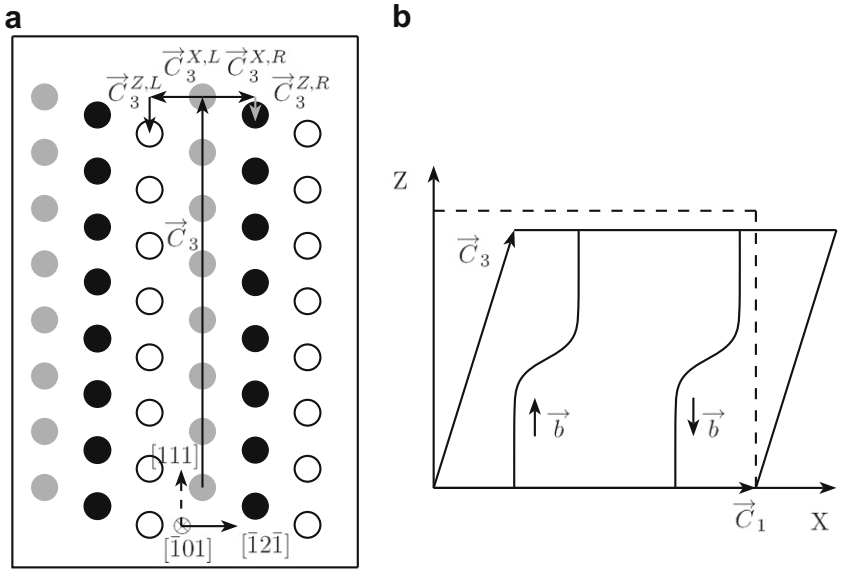

Fig. 2. Construction of periodic supercells for calculations with a single kink per dislocation line. (a) Atomistic view showing the components added to the $\vec{C}_3$ cell vector to satisfy the crystalline and defect periodicity. R refers to right and L to left. Atoms depicted in the same color belong to equivalent {1 1 1} planes. (b) Projection on the (x,z) plane of the unit cell and cell vectors compared to the cell for straight dislocation calculation (dashed line).

advanced type of potential, which accounts for magnetic effects, has been recently proposed by Dudarev and Derlet [17]. However tests performed on the existing parameterization for Fe, revealed – at variance with DFT calculations – a degenerate core structure and a shoulder in the generalized stacking fault energy surfaces. For these reasons this potential is less appropriate than the Ackland–Mendelev potential for dislocation studies. The Ackland–Mendelev potential does not account directly for magnetic effects, but changes in the local magnetic moment are expected to be small for screw dislocations because the coordination and bond length are less affected than for other defects such as vacancies, interstitials or surfaces.

Information on the structure of the kinks can be obtained from the position of the dislocation in the cell for a given value of z. We have defined a cost function based on the Volterra elastic field to determine the center (x_1,y_1) and (x_2,y_2) of the two dislocations for each {1 1 1} plane:

$$f(x_1,y_1,x_2,y_2)=\sum_{i=1}^{n}(\delta z_i-\delta^{\mathrm{el}}z_i(x_1,y_1,x_2,y_2))^2, \quad (1)$$

where $\delta^{\mathrm{el}}z_i(x_1,y_1,x_2,y_2)$ is the isotropic elastic displacement field of atom i due to the dislocation dipole positioned at (x_1,y_1) and (x_2,y_2) and δz_i is the actual atomic displacement.

The calculations have been performed using the molecular dynamics code developed by J.P. Crocombette (CEA/Saclay, France) and co-workers. Relaxations are performed using the conjugate gradient algorithm. The cell sizes range from 4b to 100b, where b is the Burgers vector (b = 2.47 Å), in the C_3 direction, and from 135 atoms/b to 1215 atoms/b for the size in the C_1 and C_2 directions.

3. Results and discussion

The kinks are initially introduced as sharp kinks. Their structures after relaxation, as obtained from Eq. (1), are represented in Fig. 3. The two types of kinks are found to have the same width, namely $w = 20b$ as defined, e.g. in Ref. [18]. This value is in very good agreement with the value of 19b proposed from an analysis of flow stress dependence on temperature and strain rates in high purity α-iron, below 250 K [19].

The convergence of the formation energy with cell-size along the dislocation line has been studied in the range from 4b to 100b (Fig. 4). From a representation as function of the inverse of the cell-size (Fig. 5), two regimes are identified: above 40b, the formation energy of the single kink has a constant value, and below 20b, it has a perfect linear dependence on the inverse of the distance between the kink and its periodic image along the dislocation line. Note that the slope is the same for the two types of kinks. Below ∼40b, it is clear from Fig. 3 that the kink has not reached its equilibrium width. In this regime of 'overlapping kinks', it can be shown that the change in line length (compared to the perfect dislocation) is proportional to the inverse of the cell-size. In a line tension model, the energy will therefore also vary as the inverse of cell-size, as observed here. Note however that the intercept has a finite value – at least for the left kink – such that another contribution to the energy should be added to the line tension. For cell sizes of 40b or more, the kink has reached its equilibrium width, which can be seen as the value minimizing the sum of the line tension energy and the Peierls contribution [18]. The fact that the energy is perfectly constant above 40b shows that the interaction between a kink and its images is negligible. The extrapolation of the linear dependence provides an upper bound value for the formation energy. A similar linear dependence was observed previously for a slightly different geometry and for other types of

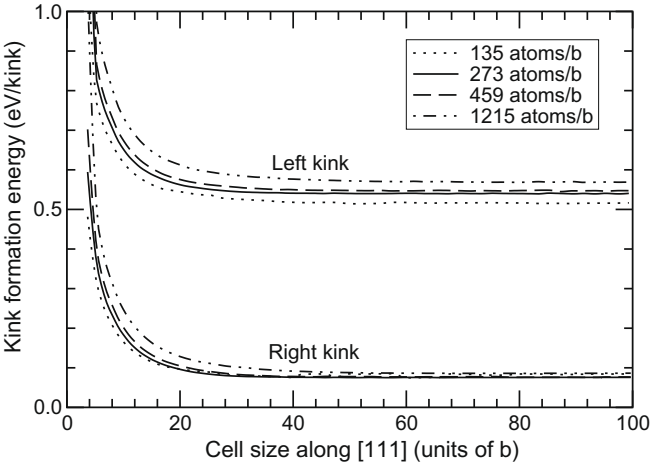

Fig. 4. Kink formation energies: convergence as a function of the cell-size along the [1 1 1] direction and number of atoms per Burgers vector.

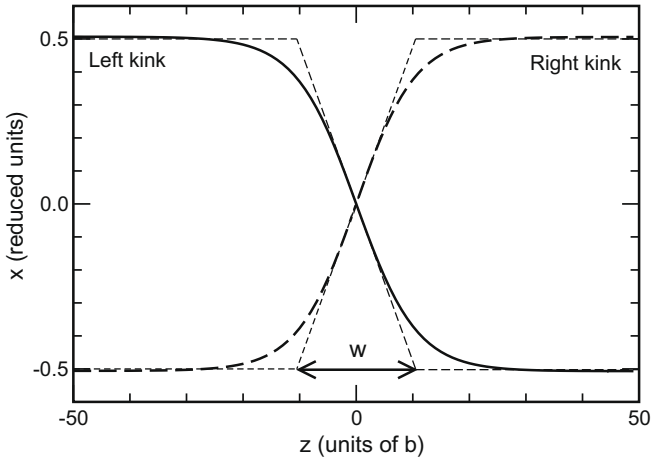

Fig. 3. Shape of the left (full line) and right (dashed line) kinks after relaxation in a cell containing 273 atoms/b in the [1 1 1] direction and 100b along the dislocation line. The positions of the dislocation are evaluated from Eq. (1), in each {1 1 1} plane along the z-axis. The displacement in the y direction is normalized to the distance between two Peierls valleys, i.e. $\sqrt{6}/3a$. The construction used to determine the kink width, w, is shown.

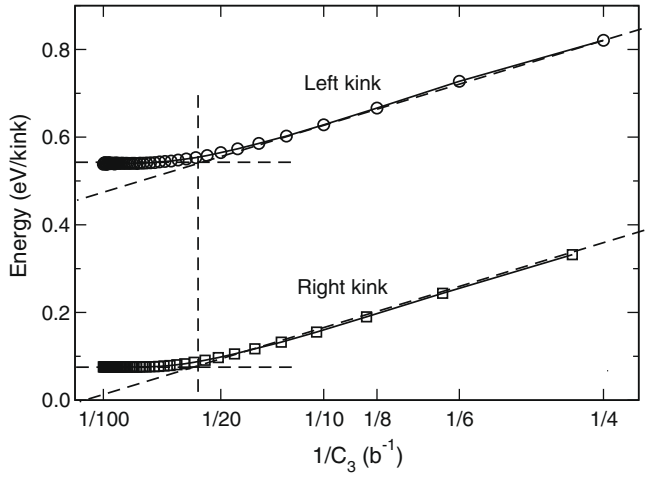

Fig. 5. Same as Fig. 3 plotted as function of inverse of cell-size in the [1 1 1] direction, represented for cells with 273 atoms/b. The horizontal dashed lines represent the constant values reached for cells larger than ∼40b.

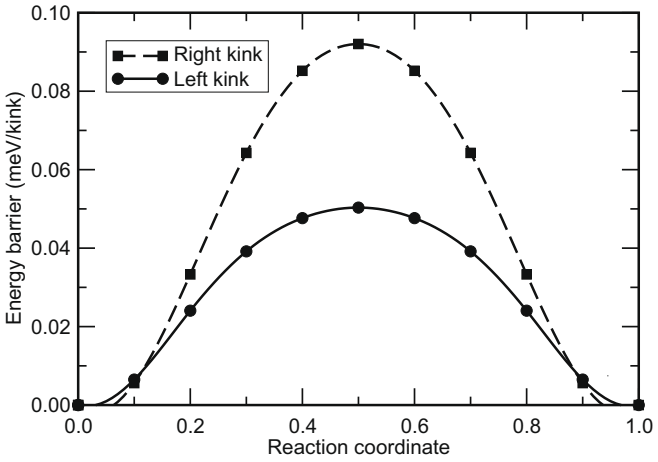

Fig. 6. Peierls potential of the second kind for the left and right kinks, calculated using the drag method in a cell containing 273 atoms/b and with 60b along the dislocation line.

dislocations [20]. However the constant value regime was not reached for the investigated cell sizes.

We have also investigated the variation of the formation energies with the distance between the dislocations, i.e. with the number of atoms per {1 1 1} plane. The change in formation energy when using cells containing from 135 to 1215 atoms/b, is found to be negligible for the right kink and less than 0.1 eV for the left kink, as shown in Fig. 4.

As a result, the values obtained for the formation energies for the right and left kinks are, respectively, 0.08 and 0.57 eV. The two types of kinks therefore have quite different formation energies. Their sum gives formation energy for a double-kink. The calculated value, 0.65 eV, is in very good agreement with the value deduced from flow stress measurements, i.e. 0.6 eV [19].

Finally, we have computed the Peierls potential for the side motion of the single kink along the dislocation line, i.e. the Peierls potential of the second kind for the two types of kinks, using the drag method [21]. The constraint used in the drag method consists in allowing the atomic positions relative to the center of mass to relax only in the hyperplane perpendicular to the vector joining the initial to the final position. The energy barriers are found to be very small, less than 0.1 meV (see Fig. 6), suggesting that both types of kink will propagate athermally along the dislocation line.

4. Conclusion

We have detailed the set up of fully periodic simulation cells to perform accurate calculations on ½⟨1 1 1⟩ screw dislocations in bcc iron using the quadrupolar distribution of dislocation dipoles, for the two types of kinks, left and right. We have described the procedure for introducing a single kink while satisfying the periodicity along the dislocation line, i.e. by removing/adding a slice of thickness $b/3$ of atoms and adding components to the cell vector along the dislocation line. This methodology was applied using the Ackland–Mendelev potential for iron. Despite the limitations of this potential concerning the description of the Peierls potential compared to DFT calculations, a good agreement is obtained with values deduced from experiments for the kink width, $w = 20b$, and the kink-pair formation energy, 0.65 eV. One of the challenges for the future is to perform similar calculations using first principles electronic structure calculation techniques in order to have more quantitative results. This has been recently achieved in Si [22] and the present results on the convergence with cell-size (parallel and perpendicular to the dislocation line) provide useful information for addressing the case of transition metals.

Acknowledgments

We acknowledge V.V. Bulatov (LLNL, USA), D. Rodney (INPG, France) and L. Proville (CEA/Saclay, France) for fruitful discussions. This work was supported by the European Fusion Materials Modelling programme and by the SIMDIM project under Contract No. ANR-06-BLAN-250.

References

[1] J. Chaussidon, M. Fivel, D. Rodney, Acta Mater. 54 (2006) 3407.
[2] C. Domain, G. Monnet, Phys. Rev. Lett. 95 (2005) 215506.
[3] G.J. Ackland, M.I. Mendelev, D.J. Srolovitz, S. Han, A.V. Barashev, J. Phys.: Condens. Matter 16 (2004) S2629.
[4] S.L. Frederiksen, K.W. Jacobsen, Philos. Mag. 83 (2003) 365.
[5] L. Ventelon, F. Willaime, J. Comput. Aided Mater. Design 14 (2008) 85.
[6] M.S. Duesbery, V. Vitek, Acta Mater. 46 (1998) 1481.
[7] W. Cai, V.V. Bulatov, J. Chang, J. Li, S. Yip, Philos. Mag. 83 (2003) 539.
[8] J. Li, C.-Z. Wang, J.-P. Chang, W. Cai, V.V. Bulatov, K.-M. Ho, S. Yip, Phys. Rev. B 70 (2004) 104113.
[9] V.V. Bulatov, J.F. Justo, W. Cai, S. Yip, Phys. Rev. Lett. 79 (1997) 5042.
[10] V.V. Bulatov, W. Cai, Computer Simulations of Dislocations, Oxford, New York, 2006.
[11] M.S. Duesbery, Acta Metall. 31 (1983) 1747.
[12] M. Wen, A.H.W. Ngan, Acta Mater. 48 (2000) 4255.
[13] G. Wang, A. Strachan, T. Çağin, J. Comput. Aided Mater. Design 8 (2001) 117.
[14] A.H.W. Ngan, M. Wen, Phys. Rev. Lett. 87 (2001) 075505.
[15] S.I. Rao, C. Woodward, Philos. Mag. A 81 (2001) 1317.
[16] G. Wang, A. Strachan, T. Çağin, Phys. Rev. B 68 (2003) 224101.
[17] S.L. Dudarev, P.M. Derlet, J. Phys.: Condens. Matter 17 (2005) 7097.
[18] J. P Hirth, J. Lothe, Theory of Dislocations, 2nd Ed., Wiley, New York, 1982.
[19] D. Brunner, J. Diehl, Phys. Stat. Sol. (a) 124 (1991) 455.
[20] N. Ide, I. Okada, K. Kojima, J. Phys.: Condens. Matter 7 (1995) 2527.
[21] G. Henkelman, G. Jóhannesson, H. Jónsson, in: S.D. Schwartz (Ed.), Theoretical Methods in Condensed Phase Chemistry, Kluwer Academic Publisher, Dordrechts, The Netherlands, 2000, p. 269.
[22] L. Pizzagalli, A. Pedersen, A. Arnaldsson, H. Jónsson, P. Beauchamp, Phys. Rev. B 77 (2008) 064106.